Polymerization Catalysts

International Edition: DOI: 10.1002/anie.201501967
German Edition: DOI: 10.1002/ange.201501967

Heterobi- and -trimetallic Ion Pairs of Zirconocene-Based Isoselective Olefin Polymerization Catalysts with $AlMe_3$**

Gabriel Theurkauff, Arnaud Bondon, Vincent Dorcet, Jean-François Carpentier, and Evgueni Kirillov**

Abstract: *The reactivity towards $AlMe_3$ of discrete cationic ansa-zirconocenes **2 a,b** that are ubiquitously used in isoselective propylene polymerization and based on [{Ph(H)C(3,6-tBu$_2$-Flu)(3-tBu-5-Et-Cp)}ZrMe$_2$)] {Cp-Flu} and rac-[{Me$_2$Si-(2-Me-4-Ph-Ind)$_2$}ZrMe$_2$] {SBI} was scrutinized. The first example of a structurally characterized Group 4 metallocene $AlMe_3$ adduct (**3 b**) is reported. In the presence of excess $AlMe_3$, the {SBI}-based $AlMe_3$ adduct **3 b** undergoes a slow decomposition via C−H activation in a bridging methyl unit to yield a new species (**4 b**) with a trimetallic {Zr(μ-CH$_2$)(μ-Me)AlMe(μ-Me)AlMe$_2$} core. EXSY NMR data for the process **2 b**⇄**3 b**→**4 b** suggest very rapid and reversible binding of an additional $AlMe_3$ molecule onto $AlMe_3$ adduct **3 b**. The resulting heterotrimetallic species intermediates exchange of methyl groups between different metal centers and slowly undergoes the C−H activation reaction towards **4 b**.*

Heterobimetallic ion pairs of the type [{LX}$_2$M(μ-R)AlR$_2$]$^+$ [A]$^-$ (where {LX}$_2$M = Group 4 metallocene-type core with R = alkyl; [A]$^-$ = counteranion, such as ["MeMAO"]$^-$, [B-(C$_6$F$_5$)$_4$]$^-$) are the cornerstone of modern olefin transformation processes, as they are recognized as dormant species and precursors of chain transfer in polymerization[1,2] and essential intermediates in carboalumination reactions.[3] Dissociation of weakly coordinated AlR_3 in the heterobimetallic ion pair, releasing a catalytically active metallocenium alkyl cation in a bare or solvated form, is considered as a prerequisite step preceding olefin coordination. In general, the stability and reactivity of these heterobimetallic species strongly depend on the nature of the counteranion and ligand and the amount of AlR_3. Though robust heterobimetallic metallocene complexes of the type [{LX}$_2$M(μ-Me)$_2$AlMe$_2$]$^+$ [B(C$_6$F$_5$)$_4$]$^{-[4,5]}$ and [{LX}$_2$M(μ-Me)$_2$AlMe$_2$]$^+$ ["MeMAO"]$^{-[6,7]}$ were documented, the post-metallocene heterobimetallic [Ti(N*t*Bu)(Me$_3$[9]aneN$_3$)(*μ*-Me)$_2$AlMe$_2$]$^+$ [B(C$_6$F$_5$)$_4$]$^-$ is, to our knowledge, the only example of a crystallographically characterized Group 4 metal $AlMe_3$ adduct reported to date.[8,9] Also, much of the reactivity of these species remains to be learnt, as revealed by recent studies.[10] Herein we report the reactivity of industrially relevant isoselective {Cp/Flu}- and {SBI}-based *ansa*-zirconocenes towards $AlMe_3$. The first solid-state structure of a metallocene $AlMe_3$ adduct, and a complex dynamic process of exchange of methyl groups mediated by formation of a heterotrimetallic bis($AlMe_3$) adduct, which eventually results in a unique C−H activation product that was only putative so far, are unveiled.

Treatment of dimethyl complexes [{Ph(H)C(3,6-*t*Bu$_2$-Flu)(3-*t*Bu-5-Et-Cp)}ZrMe$_2$] (**1a**; "{Cp-Flu}") and *rac*-[{Me$_2$Si-(2-Me-4-Ph-Ind)$_2$}ZrMe$_2$] (**1b**; "{SBI}") with 1 equiv of [Ph$_3$C]$^+$ [B(C$_6$F$_5$)$_4$]$^-$ in a [D$_8$]toluene/*o*-F$_2$-benzene mixture (8:2 *v*/*v*)[11] at room temperature, followed by addition of 2–14 equiv of $AlMe_3$,[12] resulted in the immediate and clean formation of the deep-blue and deep-red cationic bimetallic adducts **3a** and **3b**, respectively (Scheme 1).

Solution NMR spectroscopic data were acquired immediately on freshly prepared samples. The room-temperature ^{1}H and ^{13}C NMR spectra indicated a C_1 symmetry for **3a** and an average C_2 symmetry on the NMR timescale for **3b** (Supporting Information, Figures S7, S9 and S11, S12). The characteristic hydrogen atoms of the terminal $AlMe_2$ and bridging Zr(μ-Me$_2$)Al groups featured high-field chemical shifts: $\delta = -0.55$, -0.66 ppm and -1.18, -1.31 ppm, respectively, for **3a**; $\delta = -1.55$ and -1.24 ppm, respectively, for **3b**.

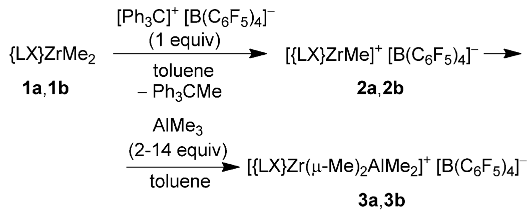

Scheme 1. Generation of $AlMe_3$ adducts **3a** and **3b**.

[*] Dr. G. Theurkauff, Dr. V. Dorcet, Prof. Dr. J.-F. Carpentier, Dr. E. Kirillov
Organometallics: Materials and Catalysis Laboratories
UMR 6226 CNRS-Université de Rennes 1
Institut des Sciences Chimiques de Rennes
35042 Rennes Cedex (France)
E-mail: jean-francois.carpentier@univ-rennes1.fr
evgueni.kirillov@univ-rennes1.fr

Dr. A. Bondon
Ingénierie Chimique et Molécules pour le Vivant
UMR 6226 CNRS-Université de Rennes 1
Institut des Sciences Chimiques de Rennes (France)

Dr. V. Dorcet
Centre de diffraction X
Institut des Sciences Chimiques de Rennes (France)

[**] This work was financially supported by Total Raffinage-Chimie (grant to G.T.). We thank Dr. J.-M. Brusson, Dr. O. Miserque, Dr. A. Vanthomme, and Dr. A. Welle (Total research) for fruitful discussions. C. Orione (CRMPO, UR1) is gratefully acknowledged for technical assistance in PGSE experiments. We are grateful to Dr. T. Roisnel and Dr. L. Toupet for assistance regarding X-ray structural studies. We thank S. Boyer (London Metropolitan University) for elemental analyses.

Supporting information for this article is available on the WWW under http://dx.doi.org/10.1002/anie.201501967.

The PGSE-derived translation diffusion coefficients for **3a** and **3b** ($D_t = 3.84(6)\times10^{-10}$ (at 28 mM) and $5.35(6)\times10^{-10}\ m^2 s^{-1}$ (at 10 mM), respectively),[13] hydrodynamic radii ($r_H = 9.02$ and 7.72 Å, respectively) and the aggregation number values calculated therefrom ($N = 1.04$ and 0.92, respectively), were all consistent with the monomeric nature of these species in solution.

All attempts to grow crystals of **3a** failed so far. However, red single crystals were reproducibly obtained and eventually isolated in 30% yield upon storing [D8]toluene/*o*-F_2-benzene solutions of **3b** at −30 °C or at room temperature. The X-ray crystallography studies performed on two different batches of such crystals that were obtained in independent experiments revealed their strict identity in terms of crystallographic parameters and composition (see the Supporting Information for details). In fact, two different species co-crystallize together as 1:1 mixed crystals of the expected heterobimetallic complex **3b** and the monocationic heterotrimetallic methylidene species **4b**·(*o*-F_2-benzene)$_2$ (Scheme 2). The latter complex **4b** is the product of a C−H activation reaction involving one of the two {Zr(μ-Me)$_2$Al} bridging methyl groups in **3b** and an additional $AlMe_3$ molecule, and implying concomitant release of a molecule of CH_4.[14] These observations are in line with previous reports and provide conclusive evidence for hypotheses made on the activation of metallocenes with MAO: 1) The observed evolution of methane from metallocene/MAO polymerization systems was proposed by Kaminsky et al.[15] to be a result of an α-hydrogen transfer reaction of the metallocene Zr−Me bonds with those Al−Me of MAO, leading to catalytically inactive Zr-CH_2-Al(Me)-O- species; 2) based on limited ^{1}H NMR spectroscopic data, Britzinger et al. surmised that, upon activation of **1b** with MAO, formation of the putative methylidene species [*rac*-{Me_2Si-(2-Me-4-Ph-Ind)$_2$}Zr(μ-CH_2)(μ-Me)AlMe_2]$^+$ ["Me-MAO"]$^-$ takes place from the corresponding parent {*rac*-[{Me_2Si-(2-Me-4-Ph-Ind)$_2$}Zr(μ-Me)$_2$AlMe_2]$^+$ ["Me-MAO"]$^-$, accompanied by concomitant evolution of methane.[7b,16] This is also reminescent to Anwander's work on the formation of Ln(μ-CH_2)Al species via C−H activation of aminomethyl group in neutral lanthanoid alkylaluminate complexes.[2c]

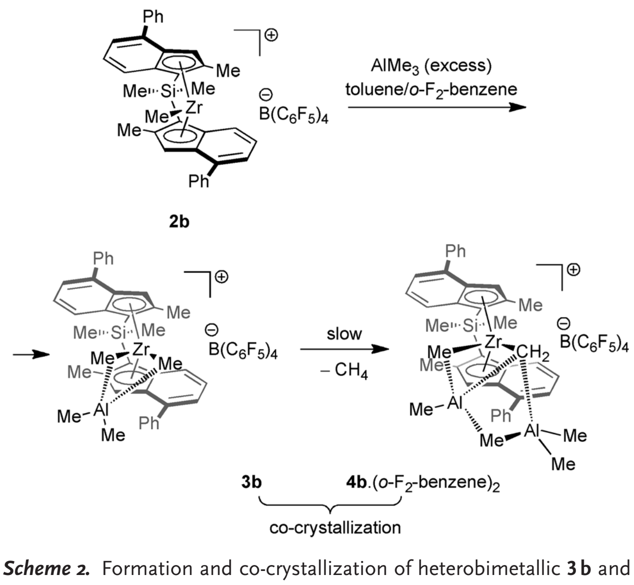

Scheme 2. Formation and co-crystallization of heterobimetallic **3b** and heterotrimetallic **4b**·(*o*-F_2-benzene)$_2$ from {SBI}-based *ansa*-zirconocenium **2b** and $AlMe_3$.

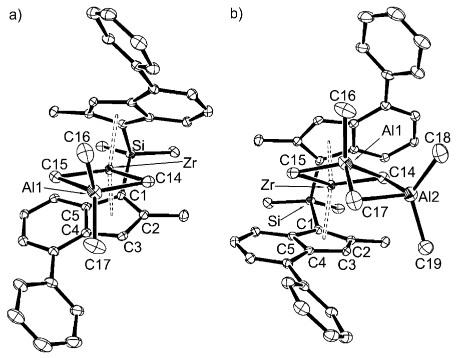

Figure 1. Crystal structures of a) [*rac*-{Me_2Si-(2-Me-4-Ph-Ind)$_2$}Zr(μ-Me)$_2$AlMe_2]$^+$ ([**3b**]$^+$) and b) [*rac*-{Me_2Si-(2-Me-4-Ph-Ind)$_2$}Zr(μ-CH_2)(μ-Me)AlMe(μ-Me)(AlMe_2)$_2$]$^+$ ([**4b**]$^+$). Ellipsoids are set at 50% probability; all hydrogen atoms, $[B(C_6F_5)_4]^-$ anion and molecules of *o*-F_2-benzene are omitted for clarity.[21]

The molecular solid-state structures of [**3b**]$^+$ and [**4b**]$^+$ are depicted in Figure 1 (selected crystallographic and geometrical parameters are given in the Supporting Information, Tables S1 and S2). Each unit cell of a mixed crystal of **3b/4b**·(*o*-F_2-benzene)$_2$ contains [**3b**]$^+$ and [**4b**]$^+$ cations with equal populations, two $[B(C_6F_5)_4]^-$ anions and two disordered *o*-F_2-benzene molecules. Although two different molecules **3b** and **4b** are present in the unit cell, the second was modeled using an element of symmetry (center of inversion; see the Supporting Information for details) applied to the first one; thus, the observed atom positions and other geometrical parameters (bond lengths and angles) are virtually the same for both **3b** and **4b**. The geometry of the central {Zr(μ-Me)$_2$Al} bimetallic core in [**3b**]$^+$ (Figure 1 a) is similar to that of the slightly dissymmetric Ti/Al analogue in the only structurally characterized $AlMe_3$ adduct of a titanium post-metallocene.[8] For instance, the Zr−Me bonds are slightly different (Zr−C14 2.350(5), Zr−C15 2.398(5) Å) while the Al1−Me bonds are identical (Al1−C14 2.106(5); Al1−C15 2.100(5) Å). Also, the latter Al1−Me distances in the bridging core are longer than the terminal distances (Al1−C16 1.934(6); Al1−C17 1.996(6) Å). In the structure of [**4b**]$^+$ (Figure 1 b), an additional bridging AlMe_2 moiety is bound with C14H_2 and C17H_3 groups, setting up a new trimetallic {Zr(μ-CH_2)(μ-Me)AlMe(μ-Me)AlMe_2} core. The Al2−Me distances (Al2−C14 1.934(6); Al2−C17 1.996(6) Å) are relatively longer as compared to those of the bimetallic [**3b**]$^+$. The Al1···Al2 distance in [**4b**]$^+$ (2.576(4) Å) is slightly above the sum of covalent radii of the aluminum atoms and is comparable to Al···Al distances observed in the Al_2Me_6 dimer (2.600–2.700 Å).[17] DFT calculations performed on species [**3b**]$^+$ $[B(C_6F_5)_4]^-$ and [**4b**]$^+$ $[B(C_6F_5)_4]^-$ entirely reproduced the experimental structures of both compounds (see the Supporting Information for details).

The insolubility of crystals of **3b/4b**·(*o*-F_2-benzene)$_2$ in toluene, even at elevated temperatures and upon addition of *o*-F_2-benzene, hampered their characterization by NMR

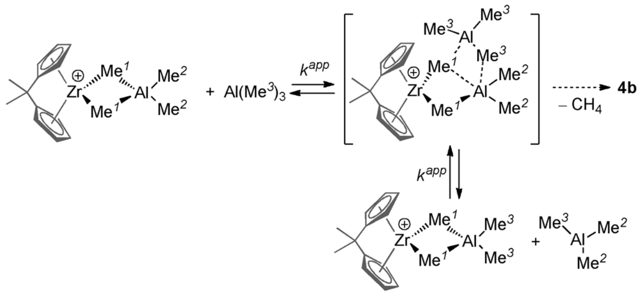

Scheme 3. The exchange process of the terminal Me/$AlMe_3$ groups observed for metallocene $AlMe_3$ adducts **3a** and **3b**.

spectroscopy. However, satisfactory combustion elemental analysis data were obtained for different, independently prepared batches of these crystals.

The dynamic behavior of $AlMe_3$ adducts **3a** and **3b** was investigated by ^1H–^1H EXSY spectroscopy on freshly prepared samples at variable temperatures in [D_8]toluene/*o*-F_2-benzene (8:2 *v*/*v*) solutions. First, the EXSY spectra recorded for systems of **3a** and **3b** with $AlMe_3$ at different mixing times (Supporting Information, Figures S10 and S17) revealed rapid exchange between the methyl groups of “free” $AlMe_3$ and those of the terminal $AlMe_2$ moieties (Scheme 3). The fact that the rates of this exchange process for both complexes **3a** and **3b** are at least one order of magnitude higher than those for the exchange between “free” $AlMe_3$ and the bridging methyl {Zr(μ-Me)$_2$Al} groups (see below) allows a dissociative mechanism involving reformation of the bare ion pairs **2a** and **2b** and “free” $AlMe_3$ to be discarded.[5] Moreover, the observed magnetization exchange constants k^{obs}_1 and k^{obs}_{-1} for both systems ($k^{app} = k^{obs}_1/[AlMe_3] = k^{obs}_{-1}/[Zr]$; see the Supporting Information) depend on the $AlMe_3$ concentration (provided the monomer/dimer equilibrium for $AlMe_3$ is very rapidly maintained on the timescale of the methyl group exchange). This suggests that the rate-determining step is the formation of heterotrimetallic intermediates (that is, **2a**·($AlMe_3$)$_2$ and **2b**·($AlMe_3$)$_2$) through reversible binding of another molecule of $AlMe_3$ with **3a** and **3b**, respectively (Scheme 3).[18] The terminal Me/$AlMe_3$ groups exchange process appeared to be substantially more facile for {SBI} complex **3b** as compared to that for its {Cp/Flu} analogue **3a**, as evaluated from the rate constants ratio $k^{app}(\mathbf{3b})/k^{app}(\mathbf{3a}) =$ ca. 140 at 298 K ([Zr] = 28.0 M; Table 1). The activation parameters for this exchange process were extracted by a standard Eyring analysis (Supporting Information, Figure S18): **3a** ([Zr] = 28.0 mM, [Al] = 55.0 mM): $\Delta H^{\neq} = 8.5(2)$ kcal mol^{-1}, $\Delta S^{\neq} = -28(2)$ cal mol^{-1} K^{-1} and $\Delta G^{\neq}_{298} = 16.70(8)$ kcal mol^{-1}; **3b** ([Zr] = 10.0 mM, [Al] = 82.0 mM): $\Delta H^{\neq} = 14.95(1)$ kcal mol^{-1}, $\Delta S^{\neq} = 3.5(1)$ cal mol^{-1} K^{-1} and $\Delta G^{\neq}_{298} = 13.93(4)$ kcal mol^{-1}. Although activation entropy values should be compared and discussed with care owing to the uncertainty in their determination,[19] the substantial difference between such values for the above exchange processes implying **3a** and **3b** likely reflects a significant difference in the nature of the respective heterotrimetallic intermediates and the associated transition states.

The two other exchange processes, namely the bridging Me/$AlMe_3$ exchange and the bridging/terminal methyl groups exchange (Supporting Information, Scheme S1), were also observed for **3a** and **3b**; they proceeded, however, with much lower rates (Supporting Information, Table S3) than those observed for the predominant terminal Me/$AlMe_3$ groups exchange (Table 1).[20] Again, the observed magnetization exchange constants (k^{obs}_1 and k^{obs}_{-1}) for both processes for **3a** and **3b** are dependent on the $AlMe_3$ concentration; this is consistent with the existence of slow bimolecular processes mediated by formation of heterotrimetallic intermediates similar to those proposed for the terminal Me/$AlMe_3$ group exchange (Scheme 3). Interestingly, only one of the two bridging methyl groups of the {Zr(μ-Me)$_2$Al} core of **3a** participates in the permutation with $AlMe_3$ (Supporting Information, Figure S11). This suggests that binding of $AlMe_3$ with the central heterometallic {Zr(μ-Me)$_2$Al} core of the C_1-symmetric molecule **3a**, leading to a heterotrimetallic adduct and enabling further exchange of methyl groups, exclusively occurs from the more open lateral site (that is, the group opposed to the *t*Bu substituent on the Cp ring).

In summary, we have synthesized and authenticated $AlMe_3$ adducts of *ansa*-zirconocenes belonging to two different families of highly isoselective propylene polymerization precatalysts, namely, the {Cp/Flu}-based **3a** and {SBI}-based **3b**. Also, we have structurally characterized the first example of a Group 4 metallocene $AlMe_3$ adduct (**3b**), as well as a product of its decomposition (**4b**), a methylidene species, which results from a C–H activation reaction of one methyl

Table 1: EXSY-derived apparent rate constants for the terminal Me/$AlMe_3$ groups exchange process for complexes **3a** and **3b**.[a]

Complex	[Zr] [mM]	[Al] [mM]	*T* [K]	Exchange of terminal Me/$AlMe_3$ groups: k^{obs}_1 and k^{obs}_{-1} [s^{-1}]	$k^{app[b]}$ [M^{-1} s^{-1}]
3a	28.0	55.0	293	0.20(1)	2.8(8)
				0.06(1)	
			298	0.19(1)	3.2(3)
				0.08(1)	
			303	0.29(2)	4(1)
				0.09(1)	
			308	0.42(2)	6(1)
				0.13(1)	
		380.0	298	0.71(1)	1.9(1)
				0.05(1)	
			303	0.97(2)	2.5(1)
				0.07(1)	
3b	10.0	82.0	278	5.81(1)	56(15)
				0.40(1)	
			283	9.4(3)	85(17)
				0.68(1)	
			288	15.9(8)	137(36)
				1.0(1)	
			298	39(2)	344(81)
				2.6(1)	
	28.0	121.0	288	26(1)	175(41)
				3.7(1)	173(5)[c]
			298	69(3)	447(127)
				9(1)	397(8)[c]

[a] Determined by ^1H–^1H EXSY NMR spectroscopy in [D_8]toluene/*o*-F_2-benzene (8:2 *v*/*v*) solutions. [b] Average value derived from $k^{app} = k^{obs}_1/[AlMe_3] = k^{obs}_{-1}/[Zr]$ (see the Supporting Information). [c] Determined from the saturation transfer experiment.

group after addition of an extra $AlMe_3$ molecule. Both products nicely co-crystallized in a mixed crystal form **3b/4b**·(*o*-F_2-benzene)$_2$. The $AlMe_3$ adducts **3a** and **3b** exhibit in solution a rapid exchange of the terminal methyl groups of $AlMe_2$ moieties and those of "free" $AlMe_3$. This process is two orders of magnitude faster for **3b** as compared to that for **3a** and is apparently mediated by the formation of hetero-trimetallic intermediates (bis($AlMe_3$) adducts **2a**·$(AlMe_3)_2$ and **2b**·$(AlMe_3)_2$, respectively). These exchange phenomena patterns may be paralleled with the much higher catalytic productivities generally observed for {SBI}-based metallocene systems in olefin polymerization processes as compared to those of their {Cp/Flu}-based congeners: We surmised that the high rate of reorganization of **3b** implying rearrangement of the $AlMe_3$ ligands in the coordination sphere of zirconium may induce larger amounts of active initiating species. Investigations along these lines are currently under way in our laboratories.

Keywords: aluminum · C–H activation · ion pairs · structure elucidation · zirconocenes

How to cite: *Angew. Chem. Int. Ed.* **2015**, *54*, 6343–6346
Angew. Chem. **2015**, *127*, 6441–6444

[1] For leading articles, see: a) M. Bochmann, *Organometallics* **2010**, *29*, 4711–4740; b) E. Y.-X. Chen, T. J. Marks, *Chem. Rev.* **2000**, *100*, 1391–1434; c) A. Valente, A. Mortreux, M. Visseaux, P. Zinck, *Chem. Rev.* **2013**, *113*, 3836–3857; d) R. Kempe, *Chem. Eur. J.* **2007**, *13*, 2764–2773.

[2] a) D. E. Babushkin, H. H. Brintzinger, *J. Am. Chem. Soc.* **2010**, *132*, 452–453; b) M. Van Meurs, G. J. P. Britovsek, V. C. Gibson, S. A. Cohen, *J. Am. Chem. Soc.* **2005**, *127*, 9913–9923. For related neutral lanthanoid-alkylaluminate complexes, see: c) L. N. Jende, C. Maichle-Mossmer, R. Anwander, *Chem. Eur. J.* **2013**, *19*, 16321–16333 and references cited therein.

[3] Topics in Organometallic Chemistry: U. M. Dzhemilev, V. A. D'yakonov, *Hydro-, Carbo- and Cycloalumination of Unsaturated Compounds in Modern Organoaluminum Reagents: Preparation, Structure, Reactivity and Use*, *Vol. 41* (Eds.: S. Woodward, S. Dagorne), Springer, Berlin, New-York, **2013**, p. 215–244.

[4] M. Bochmann, S. J. Lancaster, *Angew. Chem. Int. Ed. Engl.* **1994**, *33*, 1634–1637; *Angew. Chem.* **1994**, *106*, 1715–1718.

[5] J. M. Camara, R. A. Petros, J. R. Norton, *J. Am. Chem. Soc.* **2011**, *133*, 5263–5273 and references cited therein.

[6] J.-N. Pédeutour, K. Radhakrishnan, H. Cramail, A. Defieux, *J. Mol. Catal. A* **2002**, *185*, 119–125 and references cited therein.

[7] a) D. E. Babushkin, H. H. Brintzinger, *J. Am. Chem. Soc.* **2002**, *124*, 12869–12873 and references cited therein; b) D. E. Babushkin, H. H. Brintzinger, *Chem. Eur. J.* **2007**, *13*, 5294–5299 and references cited therein.

[8] a) P. D. Bolton, E. Clot, A. R. Cowley, P. Mountford, *Chem. Commun.* **2005**, 3313–3315; b) P. D. Bolton, E. Clot, A. R. Cowley, P. Mountford, *J. Am. Chem. Soc.* **2006**, *128*, 15005–15018.

[9] For the crystal structure of $[\{SBI\}Zr(\mu\text{-}H)_3(Al\textit{i}Bu_2)_2]^+$ $[B(C_6F_5)_4]^-$, see: S. M. Baldwin, J. E. Bercaw, L. M. Henling, M. W. Day, H. H. Brintzinger, *J. Am. Chem. Soc.* **2011**, *133*, 1805–1813.

[10] a) T. N. Lenton, J. E. Bercaw, V. N. Panchenko, V. A. Zakharov, D. E. Babushkin, I. E. Soshnikov, E. P. Talsi, H. H. Brintzinger, *J. Am. Chem. Soc.* **2013**, *135*, 10710–10719; b) D. E. Babushkin, V. N. Panchenko, H. H. Brintzinger, *Angew. Chem. Int. Ed.* **2014**, *53*, 9645–9649; *Angew. Chem.* **2014**, *126*, 9799–9803.

[11] $AlMe_3$ adducts **3a** and **3b** are poorly soluble in neat toluene, and addition of polar *o*-F_2-benzene is required to ensure complete solubility: C. Alonso-Moreno, S. J. Lancaster, C. Zuccaccia, A. Macchioni, M. Bochmann, *J. Am. Chem. Soc.* **2007**, *129*, 9282–9283.

[12] Compounds **3a** and **3b** were not produced quantitatively if only 1 equiv of $AlMe_3$ relative to Zr was used. It was originally reported that $[AlMe_3]/[Zr]$ ratios of 1.00–1.05:1 are sufficient for complete conversion of ion-pairs $[Cp_2MMe]^+$ $[B(C_6F_5)_4]^-$ into the corresponding adducts $[Cp_2M(\mu\text{-}Me)_2AlMe_2]^+$ $[B(C_6F_5)_4]^-$.[4] In later studies, however, much larger excess (typically 5–20 equiv of $AlMe_3$ versus metallocene) was eventually used to quantitatively generate the corresponding $AlMe_3$ adducts.[5] In a regular olefin polymerization experiment, co-catalyzed with commercial MAO (containing up to 30 mol% of $AlMe_3$), $[AlMe_3]/[M]$ ratios larger than 50–100 are typically used.

[13] Owing to the better solubility of metallocenium ion pair **3a**, its concentration can be maintained several times higher than that of **3b**.

[14] Actual formation of methane in the transformation of **3b** into **4b** was evidenced by ^{1}H NMR monitoring ($\delta = 0.18$ ppm in $[D_8]$toluene) of solutions of **3b** stored over long periods of time at room temperature in sealed NMR tubes. See: a) G. R. Fulmer, A. J. M. Miller, N. H. Sherden, H. E. Gottlieb, A. Nudelman, B. M. Stoltz, J. E. Bercaw, K. I. Goldberg, *Organometallics* **2010**, *29*, 2176–2179; Note that C–H activation and concomitant release of methane can be surprisingly facile in some cationic zirconocenes; see for example: b) M. Bochmann, T. Cuenca, D. T. Hardy, *J. Organomet. Chem.* **1994**, *484*, c10–c12.

[15] W. Kaminsky, A. Bark, R. Steiger, *J. Mol. Cat.* **1992**, *74*, 109–119.

[16] This observation also parallels the reactivity reported for $[CpTi(Me)_2(N{=}PR_3)]$ complexes with respect to $AlMe_3$: J. E. Kickham, F. Guerin, J. C. Stewart, D. W. Stephan, *Angew. Chem. Int. Ed.* **2000**, *39*, 3263–3266; *Angew. Chem.* **2000**, *112*, 3406–3409.

[17] a) R. G. Vranka, L. A. Elmer, *J. Am. Chem. Soc.* **1967**, *89*, 3121–3126; b) G. S. Mcgrady, J. F. C. Turner, R. M. Ibberson, M. Prager, *Organometallics* **2000**, *19*, 4398–4401.

[18] S. Lieber, M.-H. Prosenc, H. H. Brintzinger, *Organometallics* **2000**, *19*, 377–387.

[19] P. J. Barrie, *Phys. Chem. Chem. Phys.* **2012**, *14*, 327–336 and references cited therein.

[20] It should be mentioned that, owing to the very different kinetic regimes for these three exchange processes, that is, quite slow for the bridging Me/$AlMe_3$ groups and the bridging/terminal methyl groups exchanges and quite fast for the terminal Me/$AlMe_3$ groups exchange, although all were monitored at the same time using a constant mixing time (experimental constraint), there is an inaccuracy in the determination of the corresponding rate constants for the two former processes. Therefore, the corresponding rates and thermodynamic parameters (ΔH^{+}, ΔS^{+}, and $\Delta G^{\ddagger}_{298}$) extracted for the two former processes (Supporting Information, Figure S20) should be used and compared with care.

[21] CCDC 1051621 (**3b/4b**·(*o*-F_2-benzene)$_2$) contains the supplementary crystallographic data for this paper. These data can be obtained free of charge from The Cambridge Crystallographic Data Centre via www.ccdc.cam.ac.uk/data_request/cif.

Received: March 2, 2015
Published online: April 7, 2015